



## A parameterization of flow separation over subaqueous dunes

Andries J. Paarlberg,<sup>1</sup> C. Marjolein Dohmen-Janssen,<sup>1</sup> Suzanne J. M. H. Hulscher,<sup>1</sup> and Paul Termes<sup>2</sup>

Received 10 August 2006; revised 13 August 2007; accepted 11 September 2007; published 29 December 2007.

[1] Flow separation plays a key role in the development of dunes, and modeling the complicated flow behavior inside the flow separation zone requires much computational effort. To make a first step toward modeling dune development at reasonable temporal and spatial scales, a parameterization of the shape of the flow separation zone over two-dimensional dunes is proposed herein, in order to avoid modeling the complex flow inside the flow separation zone. Flow separation behind dunes, with an angle-of-repose slip face, is characterized by a large circulating leeside eddy, where a separation streamline forms the upper boundary of the recirculating eddy. Experimental data of turbulent flow over two-dimensional subaqueous bed forms are used to parameterize this separation streamline. The bed forms have various heights and height to length ratios, and a wide range of flow conditions is analyzed. This paper shows that the shape of the flow separation zone can be approximated by a third-order polynomial as a function of the distance away from the flow separation point. The coefficients of the polynomial can be estimated, independent of flow conditions, on the basis of bed form shape at the flow separation point and a constant angle of the separation streamline at the flow reattachment point.

**Citation:** Paarlberg, A. J., C. M. Dohmen-Janssen, S. J. M. H. Hulscher, and P. Termes (2007), A parameterization of flow separation over subaqueous dunes, *Water Resour. Res.*, 43, W12417, doi:10.1029/2006WR005425.

### 1. Introduction

[2] Flow over sandy river beds often leads to the formation of a regular bed morphology such as dunes [e.g., Allen, 1968; Best, 2005]. Because of flow separation and associated energy dissipation, dunes significantly influence flow resistance [e.g., Vanoni and Hwang, 1967; Wijnbenga, 1990; Ogink, 1988; Julien et al., 2002]. For many water management purposes it is of great importance to enable prediction of dune dimensions and the resulting flow resistance, especially during floods.

[3] To simulate turbulent flow over dunes numerically, the bed is often assumed to be rigid and nonerodible. However, increasing computational power has recently led to the development of morphodynamic models treating the flow, bed morphology, and sediment transport in a coupled manner. Tjerry and Fredsøe [2005] calculate dune dimensions and shapes of solitary dunes by relating sediment transport to the time-averaged bed shear stress. Nelson et al. [2005] have shown that a large-eddy simulation model with nonhydrostatic pressure and a rigid lid water surface boundary, in combination with a sediment transport model taking turbulent fluctuations of the bed shear stress into account, realistically models dune development. In continuation of this work, Giri and Shimizu [2006] improved the model of

Nelson et al. [2005] by using flow equations with the unsteady term retained and a free water surface condition. Although model results are promising, a disadvantage of these numerical models is their complexity regarding solving the flow field, especially when the flow has to be calculated repeatedly for each bed morphology update. Furthermore, it is yet infeasible to yield simulations with flood waves and long domains.

[4] In their morphodynamic model, Jerolmack and Mohrig [2005] excluded the necessity of computing the flow field by assuming a nonlinear relationship between the local bed shear stress and bed topography. To reduce the required computational effort, Onda and Hosoda [2004] used a depth-averaged hydrostatic flow model, including vertical acceleration terms, to simulate dune development. Although Jerolmack and Mohrig [2005] and Onda and Hosoda [2004] were able to simulate dune morphology over long domains, flow separation and its effects on the flow field and sediment transport were not included in their simulation models. However, there are several indications that flow separation, and associated turbulence and shear layer formation, is important for dune morphodynamics [e.g., Nelson et al., 1995; Bennett and Best, 1995; Walker and Nickling, 2002; Sumer et al., 2003].

[5] Hulscher and Dohmen-Janssen [2005] argued that offshore sand waves and river dunes are similar features, with respect to their dimensions and processes responsible for their formation. Paarlberg et al. [2005] applied a model, originally developed to predict the dimensions of offshore sand waves [see Van den Berg and Van Damme, 2005], to river conditions. The flow model is based on the two-

<sup>1</sup>Department of Water Engineering and Management, University of Twente, Enschede, Netherlands.

<sup>2</sup>HKV Consultants, Lelystad, Netherlands.

**Table 1.** Flow Conditions, Bed Form Specifications, and Results of Data Analysis for the Experiments Used in This Paper

Authors <sup>a</sup>	Flow Conditions					Bed Form Specifications				Parameterization					
	$b$ , m	$h$ , m	$U$ , m s <sup>-1</sup>	Fr	Re, $\times 10^5$	$H_d$ , m	$H_b$ , m	$L_d$ , m	$\tan\alpha_s$	$N_p$	$R^2$	$L'_{st}$	$\tan\alpha_{rt}$	$\mu_p$	$\sigma_p$
ML2	0.90	0.16	0.39	0.31	0.62	0.04	0.04	0.81	0.00	8	0.97	4.79	-0.52	0.092	0.082
ML3	0.90	0.55	0.28	0.12	1.53	0.04	0.04	0.81	0.00	7	0.99	4.69	-0.57	0.072	0.087
ML4	0.90	0.16	0.38	0.30	0.60	0.04	0.04	0.41	0.00	7	0.99	4.65	-0.62	0.064	0.066
ML5	0.90	0.16	0.20	0.16	0.32	0.04	0.04	0.41	0.00	8	1.00	5.04	-0.52	0.034	0.020
ML6	0.90	0.30	0.54	0.31	1.62	0.04	0.04	0.41	0.00	7	1.00	4.45	-0.59	0.116	0.094
ML7	0.90	0.56	0.24	0.10	1.34	0.04	0.04	0.41	0.00	7	0.96	4.55	-0.67	0.056	0.103
MR5	1.50	0.25	0.44	0.28	1.11	0.08	0.08	1.60	0.00	6	0.99	5.43	-0.61	-0.081	0.081
MR6	1.50	0.33	0.55	0.30	1.84	0.08	0.08	1.60	0.00	4	0.99	5.29	-0.51	-0.008	0.039
Te1	0.50	0.23	0.50	0.33	1.16	0.06	0.06	0.50	0.00	2	1.00	3.86	-0.52	0.211	0.435
Te2	0.50	0.23	0.50	0.33	1.16	0.06	0.06	0.50	0.00	2	1.00	4.75	-0.42	0.114	0.173
Ne1	0.70	0.20	0.51	0.37	0.99	0.04	0.04	0.80	0.00	4	0.86	3.90	-0.51	0.310	0.150
Ko3a	1.50	0.68	0.59	0.23	4.00	0.15	0.15	3.75	0.00	2	n/a <sup>b</sup>	5.03	-0.40	0.084	0.062
Ko3b	1.50	0.66	0.81	0.32	5.33	0.15	0.15	3.75	0.00	2	n/a	5.04	-0.40	0.092	0.048
Ko2a	1.50	0.68	0.66	0.26	4.53	0.15	0.13	3.75	-0.08	3	0.92	5.01	-0.24	-0.036	0.126
Ko2b	1.50	0.67	0.66	0.26	4.41	0.15	0.13	3.75	-0.08	3	0.96	5.17	-0.23	-0.139	0.092
Ko1a	1.50	0.68	0.67	0.26	4.56	0.15	0.10	3.75	-0.16	2	n/a	3.88	-0.20	0.076	0.019
Ko1b	1.50	0.67	0.66	0.26	4.45	0.15	0.10	3.75	-0.16	2	n/a	4.11	-0.17	0.046	0.061
BB1	0.30	0.10	0.57	0.58	0.57	0.05	0.04 <sup>c</sup>	0.67	-0.10	10	0.76	4.47	-0.51	-0.105	0.092
Bu1	0.61	0.05	0.51	0.75	0.24	0.01	0.01 <sup>d</sup>	0.05	-0.10	5	0.65	4.38	-0.26	0.073	0.104
NN1	0.30	0.06	0.14	0.19	0.08	0.02	0.02	n/a	0.00	5	0.99	6.69	-0.43	-0.336	0.295
NN3	0.30	0.11	0.22	0.22	0.23	0.02	0.02	n/a	0.00	5	0.98	5.78	-0.36	-0.012	0.102
Ra1	0.50	1.19	1.31	0.38	15.54	0.91	0.91	n/a	0.00	7	0.98	5.80	-0.76	-0.235	0.132
EK1	0.15	0.20	0.26	0.19	0.52	0.01	0.01	n/a	0.00	4	1.00	5.06	-0.64	-0.040	0.013

<sup>a</sup>Used numbers refer to numbering used by authors. See the notation section for parameters. ML is *McLean et al.* [1999]; MR is *Van Mierlo and De Ruiter* [1988]; Te is *Termes* [1984]; Ne is *Nelson et al.* [1993]; Ko is *Kornman* [1995]; BB is *Bennett and Best* [1995]; Bu is *Buckles et al.* [1984]; NN is *Nakagawa and Nezu* [1987]; Ra is *Raudkivi* [1963]; and EK is *Etheridge and Kemp* [1978].

<sup>b</sup>N/a means not applicable.

<sup>c</sup>Brink point is assumed at  $x = 0.05$  m,  $z = 0.041$  m in author's data.

<sup>d</sup>Brink point is assumed at  $x = 0.0025$  m,  $z = 0.01$  m in author's data.

dimensional vertical (2-DV) hydrostatic shallow water equations with a constant eddy viscosity over the flow depth and with bed load sediment transport included using a Meyer-Peter-Müller type of equation. It was shown that in cases without flow separation, dune development could be reproduced qualitatively. However, because of the hydrostatic pressure assumption, flow separation could not be captured by the model. To enable simulation of dune development from an initial disturbance to fully grown equilibrium dunes, flow separation therefore needs to be taken into account in any morphodynamic model.

[6] To predict the evolution of solitary aeolian desert dunes, *Kroy et al.* [2002] included a parameterization of flow separation in their morphodynamic model. *Kroy et al.* [2002] parameterized the shape of the separation streamline, which forms the upper boundary of the flow separation zone, on the basis of numerical computations of air flow over bed forms. The flow was computed using the separation streamline as an artificial “bed” in the region of flow separation, effectively avoiding the necessity of modeling the complicated flow behavior inside the flow separation zone.

[7] To keep computational effort to a minimum but to retain the process of flow separation in a simple manner in the morphodynamic model of *Paarlberg et al.* [2005], a similar approach to that adopted by *Kroy et al.* [2002] can be used. The present paper will analyze whether the shape of the flow separation zone can be parameterized in the case of water flow over bed forms. To this end, experiments of turbulent flow over 2-D subaqueous bed forms are analyzed, with different bed form heights and aspect ratios

(ratio of dune height to dune length) and under various flow conditions.

[8] In section 2 an overview of the data used in this paper is given, and velocity profiles are analyzed to determine the shape of the flow separation zone for the different experiments. In section 3 the separation streamline is parameterized using a third-order polynomial function, which is fitted to the individual experiments. The parameters or bed form properties controlling the dimensions of the flow separation zone are then investigated, resulting in an estimate of the length of the flow separation zone based on bed form properties. This allows imposition of the shape of the separation streamline, both at the flow separation point and at the flow reattachment point. The paper shows that the shape of the flow separation zone can be estimated independently of flow conditions using solely bed form properties.

## 2. Flow Separation

### 2.1. Used Data Sets

[9] The parameterization of the separation streamline requires detailed measurements of the reverse flow near the bed inside the flow separation zone, and hence only flume data are detailed enough to use for the parameterization. The data used in the present paper are summarized in Table 1 and consist of (1) dunes with a horizontal bed at the flow separation point, (2) dunes with a negative slope at the flow separation point, and (3) backward facing steps. All measurements comprise time-averaged velocity data.

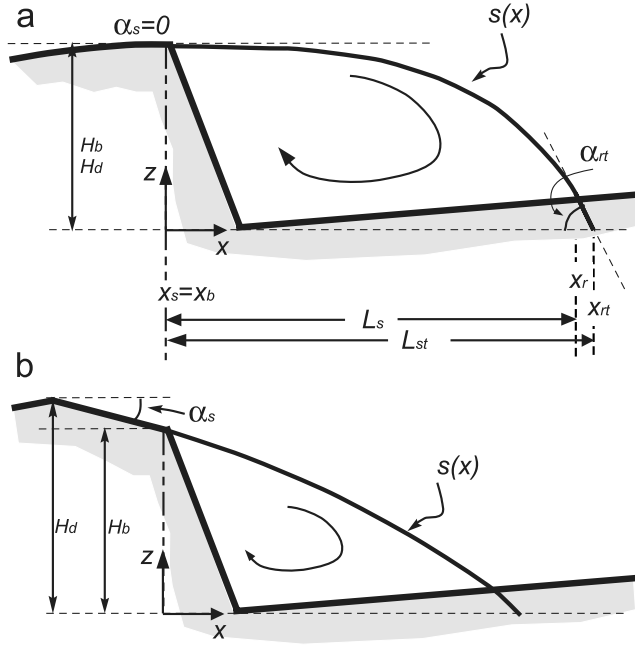


**Figure 1.** Schematic representation of flow separation in the lee of a dune with (a) horizontal bed at the flow separation point and (b) negative bed slope at the flow separation point, including a sketch of the separation streamline. Flow separation is assumed to occur at the brink point ( $x_b$ ). See the notation section for used parameters.

[10] In cases where bed load transport is dominant, dunes are often asymmetric, with a leeside slope at the angle of repose ( $\sim 30^\circ$ ) and a region of permanent flow separation in the lee (Figure 1a) [Smith and McLean, 1977; Kostaschuk and Villard, 1996; Best, 2005]. Part of the data used consists of flume experiments with such dunes [Termes, 1984; Van Mierlo and De Ruiter, 1988; Nelson et al., 1993; McLean et al., 1999]. In nature, however, dunes are often of more complex shape. Therefore dunes with negative slopes at the brink point, the point where the leeside slope suddenly changes to the angle of repose (Figure 1b), are also included [Buckles et al., 1984; Kornman, 1995; Bennett and Best, 1995]. Since flow separation over backward facing steps is largely similar to that over dunes with angle-of-repose slip faces, experiments with backward facing steps are also included in the analysis [Raudkivi, 1963; Nakagawa and Nezu, 1987; Etheridge and Kemp, 1978].

[11] For the experiments with backward facing steps the separation point is located at the edge of the step. In the case of dunes, separation is assumed to occur at the brink point. For most experiments this point is clearly defined, except for the experiments of Buckles et al. [1984] and Bennett and Best [1995]. For these two experiments the location of the brink point is estimated at the point where the bed slope is about  $-6^\circ$  by analyzing the point where the leeside slope has the sharpest decline (exact locations can be found in Table 1).

**2.2. Shape of the Flow Separation Zone**

[12] Inside the flow separation zone a recirculation eddy with reverse flow near the bed is present. This means that

the net discharge through a vertical cross section between the bed and the separation streamline is zero. In other words, the upstream directed discharge between the bed and the point of zero velocity is equal to the downstream directed discharge between the point of zero velocity and the separation streamline. On the basis of this assumption the vertical position of the separation streamline ( $z = z_{sep}$ ) is found from

$$\int_{z_b}^{z_{sep}} u(z) dz = 0, \tag{1}$$

where  $z$  is the vertical coordinate, with the bed at  $z = z_b$ .

[13] Figure 2 shows cubic interpolated velocity data, the points of zero velocity (i.e.,  $u(z) = 0$ ), and the separation streamline for experiment T5 of Van Mierlo and De Ruiter [1988] (computed  $z_{sep}$  values are linearly connected for clarity). It should be noted that measurements over the steep leeside slope of dunes are least detailed and that extrapolation over a significant portion of the velocity profile within the flow separation zone must be made. This leads to the highest uncertainty in the location of the separation streamline ( $z_{sep}$ ) over the leeside slope.

[14] Kroy et al. [2002] parameterize the shape of the separation streamline by imposing a smooth connection at both the flow separation and reattachment point. They estimated the length of the flow separation zone ( $L_s$ ) on the basis of a predefined maximum slope of the separation streamline ( $-14^\circ$ ). Since Kroy et al. [2002] studied solitary dunes, the flow reattachment point occurs on a flat bed. In Figure 2 the parameterization of Kroy et al. [2002] for the shape of the separation streamline is included. For most of the experiments analyzed in the present paper, and especially when the bed is horizontal at the flow separation point (i.e.,  $\alpha_s = 0$ , Figure 1a), the parameterization of Kroy et al. [2002] turns out to fit the zero velocity data instead of the separation streamline. This is mainly caused by the assumptions of Kroy et al. [2002] that the length of flow separation is found from imposing a maximum slope of the separation streamline and that the separation streamline smoothly connects to a flat bed at the reattachment point.

**3. Parameterization of the Separation Streamline**

[15] In this section a separation streamline  $s(x)$  is determined for each individual experiment by fitting a third-order

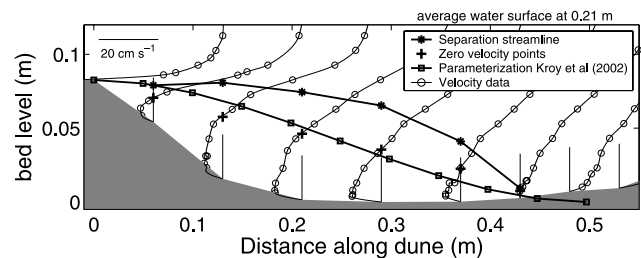


**Figure 2.** Illustration of velocity data, zero velocity points, and separation streamline for experiment T5 of Van Mierlo and De Ruiter [1988]. The separation streamline is compared to the parameterization of Kroy et al. [2002].

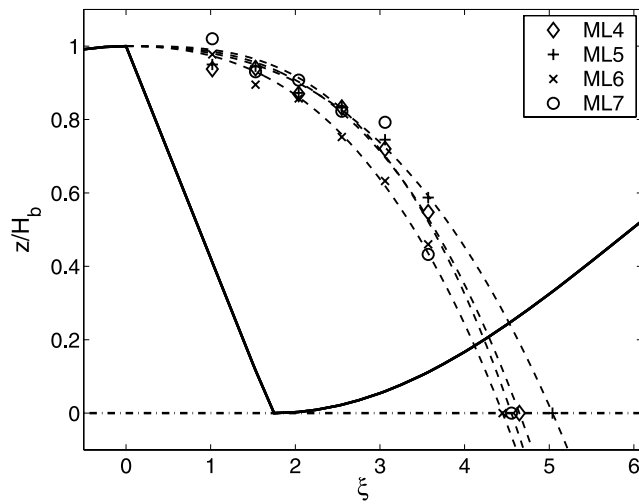


**Figure 3.** Separation streamlines for data of *McLean et al.* [1999]. Dashed lines are the regressed separation streamlines (symbols at trough elevation distinguish the four experiments).

polynomial function in  $x$ , the distance from the flow separation point, to the vertical locations  $z = z_{\text{sep}}$  found from equation (1). To enable comparison between the experiments, both the longitudinal coordinate  $x$  and the vertical coordinate  $z$  are scaled against the brink point height of a bed form ( $H_b$ ). Once the separation streamline is known, the reattachment point can be determined, and which parameters control the length of the flow separation zone is investigated.

### 3.1. Determination of Separation Streamline

[16] The separation streamline is parameterized using the same third-order polynomial function as used by *Kroy et al.* [2002]:

$$\tilde{s}(\xi) = \frac{s(\xi)}{H_b} = s_3\xi^3 + s_2\xi^2 + s_1\xi + s_0, \quad (2)$$

where  $\xi = (x-x_s)/H_b$  and  $s_0 \dots s_3$  are coefficients. The shape of the separation streamline, as illustrated in Figure 2, can be approximated by imposing a smooth connection of the separation streamline to the bed at the flow separation point ( $\xi = 0$ ), yielding for coefficients  $s_0$  and  $s_1$

$$s_0 = \tilde{s}(0) = 1 \quad (3)$$

$$s_1 = \frac{d\tilde{s}(0)}{d\xi} = \tan \alpha_s. \quad (4)$$

[17] *Kroy et al.* [2002] imposed two conditions at the flow reattachment point as well; however, in our case the flow reattachment point is not known a priori. Therefore the coefficients  $s_2$  and  $s_3$  are fitted to the vertical locations  $z = z_{\text{sep}}$  found from equation (1). The fitting procedure results in a separation streamline for each individual experiment, and Figure 3 shows the results for four experiments of *McLean et al.* [1999].

[18] For the experiment of *Termes* [1984] and *Kornman* [1995] it was necessary to set coefficient  $s_3$  to zero in

equation (2) since too few velocity profiles are located within the flow separation zone. For the experiments of *Buckles et al.* [1984] and *Nelson et al.* [1993] it was also necessary to use  $s_3 = 0$  since otherwise no monotonic decreasing regression line was found, and consequently, no reattachment point could be found.

[19] To use the parameterized separation streamline in a morphodynamic model, it is important to describe the shape of the separation streamline correctly. This paper shows that the shape of the separation zone is captured with sufficient accuracy using a third-order polynomial function, with coefficients  $s_0$  and  $s_1$  set by realistic boundary conditions, and setting coefficients  $s_2$  and  $s_3$  using regression analysis. The observed behavior that the separation streamline reattaches downstream at a certain angle (Figure 2) is also captured by the parameterization.

[20] Table 1 lists the coefficients of determination for the fitted separation streamlines ( $R^2$ ). Especially for the experiments of *McLean et al.* [1999] and *Van Mierlo and De Ruiter* [1988] and experiments with backward facing steps, good fits are obtained. By using a second-order polynomial function, the overall shape of the separation zone could not be captured, especially near the region of flow reattachment. Extending the parameterization to a fourth-order polynomial function yielded unrealistic separation zone shapes since the extra fitting coefficient led to fitting noise rather than the average shape of the flow separation zones. *Schatz and Herrmann* [2006] used an elliptical function to parameterize the separation streamline for air flow over aeolian dunes. Their method also requires four coefficients; however, to set these coefficients, the reattachment point has to be known a priori.

### 3.2. Determination of the Flow Reattachment Point

[21] For each experiment the shape of the flow separation zone is now known, allowing determination of the (time-averaged) location of the flow reattachment point. However, since the experiments used in this paper are performed with different bed form geometries (i.e., different bed form heights and/or lengths, Table 1), the bed slope at the flow reattachment point is not equal between the different experiments. To be able to compare the various experiments, a location  $x_{\text{rt}}$  is defined, where the cubic separation streamline would intersect a flat bed whose elevation is the same as the trough elevation (Figure 1a). This defines the separation zone length  $L_{\text{st}} = x_{\text{rt}} - x_s$  and a nondimensional separation zone length  $L'_{\text{st}} = L_{\text{st}}/H_b$ . The angle of the separation streamline with the hypothetical flat bed (dashed lines in Figures 1a and 1b that have the same elevation as the trough) is defined as  $\tan \alpha_{\text{rt}}$ . At the reattachment point ( $\xi = L'_{\text{st}}$ ) this yields

$$\tilde{s}(L'_{\text{st}}) = 0 \quad (5)$$

$$\frac{d\tilde{s}(L'_{\text{st}})}{d\xi} = \tan \alpha_{\text{rt}}. \quad (6)$$

Combining this equations (2)–(4) yields at  $\xi = L'_{\text{st}}$

$$s_3L'^3_{\text{st}} + s_2L'^2_{\text{st}} + \tan \alpha_s L'_{\text{st}} + 1 = 0 \quad (7)$$

$$3s_3L'^2_{\text{st}} + 2s_2L'_{\text{st}} + \tan \alpha_s = \tan \alpha_{\text{rt}}. \quad (8)$$

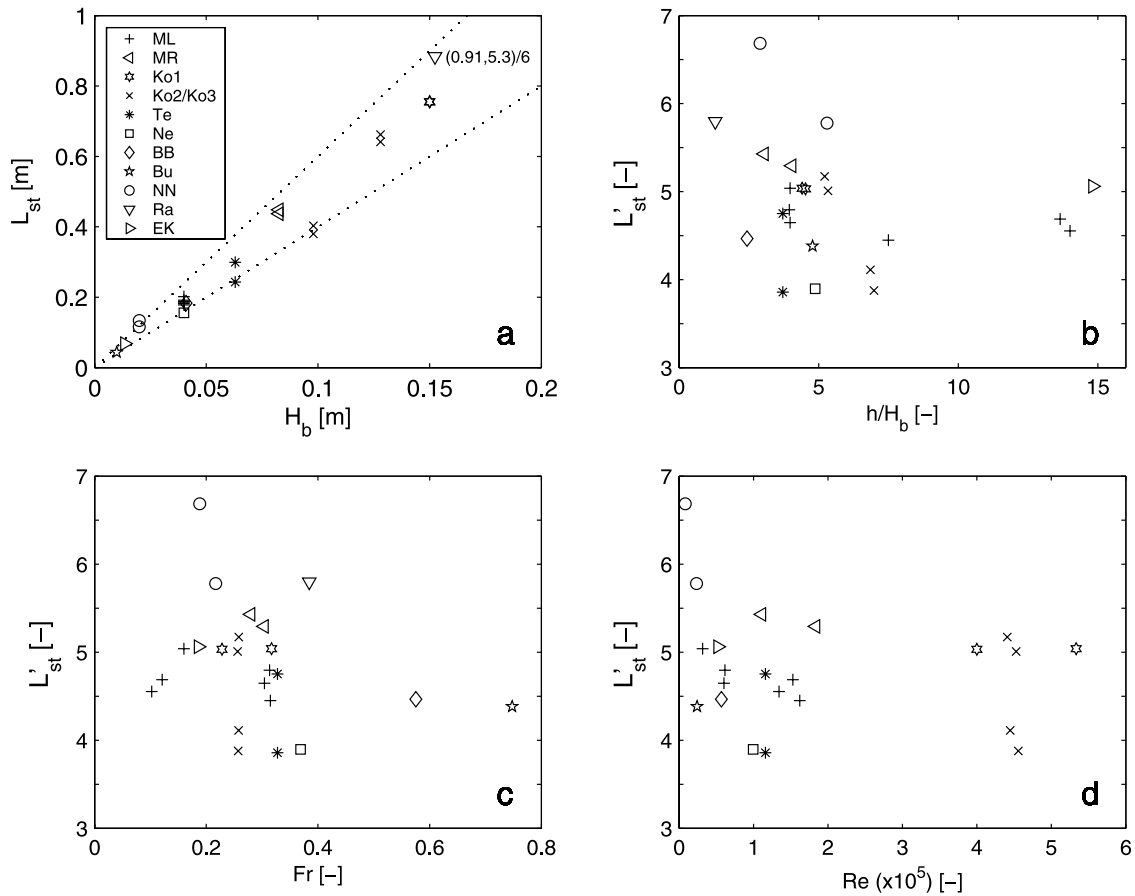


**Figure 4.** (a) Relationship between the brink point height and the (dimensional) separation zone length (see Figure 1 and the notation section for parameters and Table 1 for abbreviations used in the legend). The data for the experiment of Raudkivi [1963] is scaled by a factor 1:6 for clarity. The dotted lines represent  $L_{st} = 4H_b$  and  $L_{st} = 6H_b$ . Dependency of the nondimensional separation zone length is shown on (b) the ratio of water depth to brink point height, (c) the Froude number, and (d) the Reynolds number.

[22] Using the fitted curves determined in section 3.1, equation (7) is solved to obtain  $L'_{st}$ , and equation (8) yields  $\tan \alpha_{rt}$  for each individual experiment. Results are summarized in Table 1, and for experiments ML4-7 the positions of  $\xi = L'_{st}$  are given in Figure 3.

### 3.3. Length of the Flow Separation Zone

[23] Figure 4 shows that the length of the flow separation zone increases for increasing brink point heights (Figure 4a) and that the nondimensional length of the flow separation zone ( $L'_{st} = L_{st}/H_b$ ) varies roughly between 4 and 6. This range is confirmed by various sources, with the nondimensional separation zone length often reported around 4–6 [e.g., Engel, 1981; Van Mierlo and De Ruiter, 1988; Niño *et al.*, 2002; Fernandez *et al.*, 2006]. Figures 4b–4d show no obvious relationship between characteristic flow parameters and the flow separation zone length. This could also be concluded from Figure 3, which shows largely identical separation streamlines for four experiments where the fixed dune shape is equal but flow conditions are different. It is also in agreement with Engel [1981], who showed experimentally that the nondimensional length of the flow separation zone is largely independent of the Froude number and the relative water depth (ratio of water depth to dune height), and with Walker and Nickling [2002], who stated

that the reattachment distance behind desert dunes only slightly increased with incident wind speed.

[24] Several authors suggest that the length of the flow separation zone is controlled, apart from brink point height, by the local bed slope at the flow separation point [Paarlberg *et al.*, 2005; Schatz and Herrmann, 2006]. Therefore Figure 5 shows the nondimensional length of the flow separation zone as a function of the local bed slope at the separation point. The experiments used in the present analysis have either a horizontal bed or a negative bed slope at the flow separation point (i.e.,  $\tan \alpha_s \leq 0$ , Table 1). Four slope classes are used, and each class is represented by a mean and its standard deviation. Linear regression through the data yields (Figure 5)

$$L'_{st} = 6.48 \tan \alpha_s + 5.17. \quad (9)$$

[25] By performing numerical simulations of air flow over fixed isolated aeolian dunes, Schatz and Herrmann [2006] also found a linear relation between the separation zone length and the bed slope at the flow separation point. Schatz and Herrmann [2006] found the nondimensional flow separation zone length to extend roughly 10–30% farther downstream than found in this paper (Figure 5). In

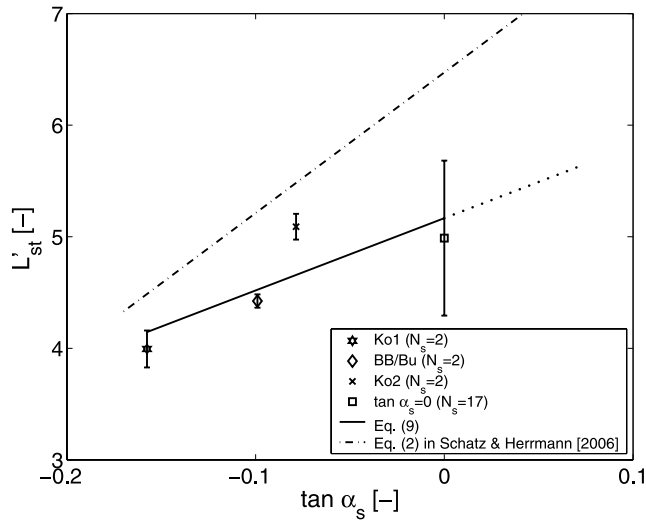


**Figure 5.** Nondimensional length of the flow separation zone ( $L'_{st}$ ) as a function of the bed slope at the flow separation point ( $\tan \alpha_s$ ). The data are grouped into four slope classes with  $N_s$ , the number of observations in that class; per class the mean and its standard deviation are shown. The solid line is a linear fit through the mean nondimensional separation zone lengths, and the dash-dotted line is equation (2) of *Schatz and Herrmann* [2006].

their conceptual model of leeside airflow, however, *Walker and Nickling* [2002] suggest that the separation zone extends farther over isolated solitary dunes than over closely spaced dunes because of decreased surface roughness. *Schatz and Herrmann* [2006] showed, using a numerical simulation, that the separation zone length over closely spaced dunes with a horizontal bed at the flow separation point (i.e.,  $\tan \alpha_s = 0$ ) is about 25% smaller than over isolated dunes. This means that for dunes with a horizontal bed, *Schatz and Herrmann* [2006] found a nondimensional separation zone length of  $L'_{st} \approx 4.85$ , which is well within the range of  $L'_{st}$  found in this paper (Figure 5).

### 3.4. Parameterization Based on Bed Form Properties

[26] The length of the flow separation zone is shown to be largely independent of flow conditions (Figures 4b–4d), but it depends on brink point height (Figure 4a) and bed slope at the flow separation point (Figure 5). Therefore the four coefficients  $s_0 \dots s_3$  are determined on the basis of bed form properties. Coefficients  $s_0$  and  $s_1$  are set using equations (3) and (4). The remaining coefficients  $s_2$  and  $s_3$  can be determined from equations (7) and (8) if the location of the reattachment point and the slope of the separation streamline at the flow reattachment point are known. The position of the flow reattachment point ( $\xi = L'_{st}$ ) can be estimated using equation (9), with the brinkpoint height and the bed slope at the flow separation point as inputs. For the coefficients  $s_2$  and  $s_3$  this yields

$$s_3 = \frac{\tan \alpha_{rt}}{L'_{st}{}^2} + \frac{\tan \alpha_s}{L'_{st}{}^2} + \frac{2}{L'_{st}{}^3} \quad (10)$$

$$s_2 = -s_3 L'_{st} - \frac{\tan \alpha_s}{L'_{st}} - \frac{1}{L'_{st}{}^2}. \quad (11)$$

[27] In the case of a horizontal bed at the flow separation point (i.e.,  $\tan \alpha_s = 0$ ) the average angle of the separation streamline at the reattachment point is  $\tan \alpha_{rt} = -0.53$  ( $\sigma = 0.11$ ), yielding  $s_3 = -5.4 \times 10^{-3}$  and  $s_2 = -9.7 \times 10^{-3}$ . In the case of a negative bed slope at the flow separation point, the angle of the separation streamline at the flow reattachment point is not known because only limited data for these cases are available. To be able to use one boundary condition less at the flow reattachment point, the coefficient  $s_3$  is set to zero in equations (10) and (11) if  $\tan \alpha_s < 0$ .

[28] The shape of the flow separation zone can now be estimated with equation (2), using equations (3), (4), and (9)–(11) to set the coefficients of the polynomial. Figure 6 compares the parameterization with the separation streamlines extracted from the experiments (section 3.1). To assess for each experiment how well the parameterization compares to the data, the relative error  $E_p$  between the measured positions of the separation streamlines ( $z_{sep}$ ) and the parameterized separation streamline ( $z_{par}$ ) is determined for each measurement point  $i$  within the flow separation zone

$$E_{p,i} = \frac{z_{par,i} - z_{sep,i}}{H_b}, \quad i = 1..N_p, \quad (12)$$

where  $N_p$  is the number of measurements within the flow separation zone (Table 1). For each experiment the mean ( $\mu_p$ ) and standard deviation ( $\sigma_p$ ) of the errors computed with equation (12) are presented in Table 1. A zero mean, together with a zero standard deviation, would imply a perfect fit; a positive mean implies that the parameterized separation streamline is on average above the fitted separation streamline. The average value of the mean error  $\mu_p$  is 0.02 ( $\sigma = 0.14$ ) with an average standard deviation  $\sigma_p$  of 0.11 ( $\sigma = 0.09$ ), meaning that the parameterization based on dune properties captures the average shape of the flow separation zone.

[29] Figure 6 shows that for dunes with a horizontal bed at the flow separation point the agreement between the data and the parameterization is fairly good, especially for the experiments of *McLean et al.* [1999] and *Van Mierlo and De Ruiter* [1988]. For backward facing steps the size of the flow separation zone is generally underestimated by the parameterization. This might be due to the fact that backward facing steps have a secondary corner eddy just downstream from the edge of the step near the bed. For dunes this secondary corner eddy is not present or is at least less pronounced because the angle of the lee is about  $-30^\circ$  instead of  $-90^\circ$  (i.e., vertical) for backward facing steps.

[30] The bottom four plots in Figure 6 consider the experiments with a negative bed slope at the flow separation point, where the coefficient  $s_3$  is set to zero. Good agreement is also observed here between the data and the parameterization.

## 4. Discussion

### 4.1. Application of the Parameterization in a 2-DV Morphodynamic Model

[31] The aim for future research is to use the proposed parameterization in a two-dimensional vertical (2-DV) dune development model where the flow is treated as hydrostatic, meaning that the details of separated flows cannot be

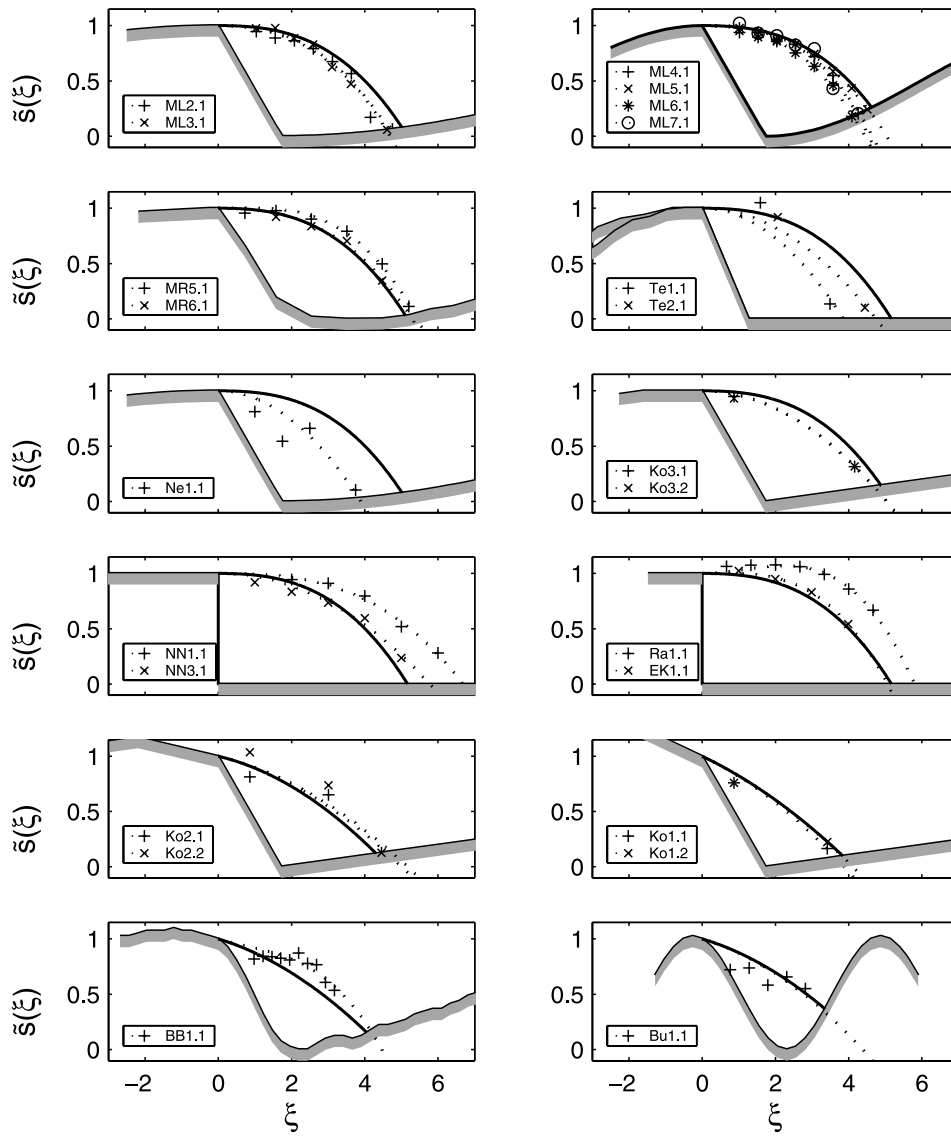


**Figure 6.** Comparison of the parameterization with the separation streamlines found from the regression analysis. Bed profiles are underlain by a gray shading for clarity. Within the flow separation zone the solid lines represent the parameterization, the symbols represent the measured vertical positions along the separation streamlines ( $z_{sep}$ ), and the dotted line represents the fitted separation streamlines to these positions.

predicted (e.g., the model described by Paarlberg *et al.* [2005]). Following the approach of Kroy *et al.* [2002], the parameterized separation streamline can be used to provide an artificial bed over which the hydrostatic assumption is approximately true. Thus only the hydrostatic flow outside the flow separation zone has to be calculated, which saves the computational effort related to modeling the flow within and around the flow separation zone.

[32] Initial results indicate that river dune migration and formation can be captured with a morphodynamic model where the flow separation zone behavior is parameterized [see Paarlberg *et al.*, 2006]. Using this approach, details related to the flow behavior within the flow separation zone, such as the shear layer developing downstream of the flow separation point [e.g., McLean *et al.*, 1999; Fernandez *et al.*, 2006], are not included. For the aeolian case, Kroy *et al.*

[2002] argue that dune migration and formation do not very sensitively depend on the flow behavior within the flow separation zone. Although the process of flow separation in unidirectional air and water flows is quite similar, future research should investigate whether it is sufficient to know solely the shape of the flow separation zone in order to facilitate predicting river dune development or if this parameterization has to be extended with details within and around (shear layer) the flow separation zone.

#### 4.2. Application of the 2-DV Parameterization to Complex River Dune Configurations

[33] The proposed parameterization estimates the shape of the flow separation zone in the leeside of straight-crested two-dimensional vertical dunes with angle-of-repose slip faces. In the field, however, often more complex dune

configurations occur. In large rivers the average leeside slope of dunes is often lower than about  $-8^\circ$  [Best, 2005]. Best and Kostaschuk [2002] showed that the flow separation zone in the leeside of a low-angle dune with a maximum leeside slope of  $-14^\circ$  is nonpermanent, with intermittent flow separation for up to 4% of the time. Additionally, river dunes often have 3-D structures, such as amplitude variations or crest line curvature. Allen [1968] illustrated flow patterns over 3-D dunes, revealing complex flow separation zone dynamics due to generated vorticity and convergence and divergence of flow [Best, 2005]. This raises the question of how to apply the proposed separation zone parameterization to low-angle dunes and 3-D dune configurations.

[34] Since low-angle dunes possess no clearly defined (or even absent) brink point, and since flow separation is nonpermanent, the 2-DV parameterization is difficult to apply to low-angle dunes. Future studies should investigate over which leeside slopes the flow separates (defining a critical bed slope) and to what extent. If this information is available, the parameterization can be applied using a critical bed slope as the brink point; in morphological calculations the flow separation zone should be ignored for the time it is not present. It should be noted that the morphodynamic model of Paarlberg *et al.* [2006] only considers bed load transport. Possibly, this assumption limits the occurrence of low-angle dunes since their occurrence may be related to the presence of suspended sediment transport [Best and Kostaschuk, 2002; Best, 2005].

[35] Recent studies by Venditti [2007] and Maddux *et al.* [2003a, 2003b] showed that the flow field over simple regular 3-D dunes is significantly different from that over their 2-D counterparts. Secondary currents and flow convergence and divergence over the 3-D shapes significantly influence the separation zone dynamics.

[36] Maddux *et al.* [2003a, 2003b] used fixed dunes which were 2-D across the flume width, having cosine-shaped stoss sides in streamwise direction and a variable height of the crest line, thereby creating a 3-D form. Equation (9) determines the separation zone length using the bed slope at the flow separation point ( $\alpha_s = 0$  in this case) and brinkpoint height as input. If the parameterization follows the main flow direction, the flow separation zone extends farther downstream over the maxima in dune height, as was found by Maddux *et al.* [2003a]. However, Maddux *et al.* [2003a] also showed that secondary currents and flow convergence and divergence over the 3-D shapes significantly influenced turbulence generation. This could be taken into account by including the lateral flow component and by applying the parameterization along streamlines instead of along the main flow direction.

[37] In the experiments of Venditti [2007] the crest line was curved but was constant in height and cross-sectional 2-D shape. For dunes where the crest center is ahead of the banks (“lobe”-shaped dunes), the flow separation zone extended farther downstream than was the case with the 2-D counterpart. In situations where the crest is behind that of the banks (“saddle”-shaped dunes), convergence of flow in the hollow in the leeside suppressed the formation of a flow separation zone, resulting in less turbulence but higher velocities. For these shapes our parameterization is inadequate since the dune height is constant in these experiments.

This suggests the importance of including streamlines and streamline curvature in the parameterization.

[38] Thus, to apply the separation zone parameterization to such 3-D river dune configurations, the 2-DV dune model should be extended to a 3-D morphodynamic model, such as the model of Hulscher [1996]. This allows investigation into how the shape of the separation zone depends on two-dimensional horizontal (2-DH) dune structures, e.g., by following streamlines and allowing for convergence and divergence of the parameterized separation zone. For natural irregular 3-D dune fields it might be necessary to derive a different parameterization, e.g., by including turbulent quantities or vorticity.

## 5. Conclusions

[39] In this paper a parameterization of flow separation associated with straight-crested subaqueous sand dunes is proposed, which can easily be applied in 2-DV morphodynamic models to avoid modeling the complex flow behavior inside the flow separation zone. The shape of the flow separation streamline can be approximated by a third-order polynomial as a function of the distance away from the flow separation point.

[40] The length of the flow separation zone is shown to be largely independent of flow conditions but depends on the brink point height and decreases when there is a negative bed slope at the brink point. A linear relationship is found between the bed slope at the flow separation point and the length of the flow separation zone, allowing estimation of the location of the flow reattachment point.

[41] The coefficients of the third-order polynomial are set using physical boundary conditions at the flow separation point and at the flow reattachment point. A smooth connection to the bed is assumed at the flow separation point. Since the angle of the separation streamline at the reattachment point is found to be almost constant, this angle is used as boundary condition at that point. The shape of the separation streamline, and thus the flow separation zone, are captured well by the proposed parameterization for dunes with different heights and height to length ratios and for a wide range of flow conditions.

## Notation

$\alpha_s$	bed slope at the flow separation point.
$\alpha_{rt}$	slope of the separation streamline at $x_{rt}$ .
$b$	flume width, m.
$E_p$	relative error of the parameterization.
Fr	Froude number.
$h$	average flow depth, m.
$H_d$	bed form height (measured from crest to trough elevation), m.
$H_b$	brink point height (measured from brink point to trough elevation), m.
$L_d$	bed form length (measured from crest to crest), m.
$L_s$	length of the flow separation zone, m.
$L_{st}$	length of the flow separation zone measured from $x_s$ to $x_{rt}$ , m.
$L'_{st}$	nondimensional length of the flow separation zone (equal to $L_{st}/H_b$ ).
$\mu_p$	mean value of $E_p$ .

$N_p$	number of points on the separation streamline to determine regression (not including the separation point).
$N_s$	number of observations in a slope class.
$R^2$	coefficient of determination.
Re	Reynolds number.
$s(x)$	separation streamline, m.
$\bar{s}(\xi)$	nondimensional separation streamline (equal to $s/H_b$ ).
$s_0 \dots s_3$	coefficients for the separation streamline.
$\sigma_p$	standard deviation of $E_p$ .
$u$	horizontal flow velocity, $\text{m s}^{-1}$ .
$U$	average horizontal flow velocity, $\text{m s}^{-1}$ .
$x$	horizontal streamwise coordinate, m.
$x_b$	$x$ coordinate of the brink point, m.
$x_r$	$x$ coordinate of the flow reattachment point, m.
$x_{rt}$	location where the separation streamline would intersect a flat bed whose elevation is the same as the trough elevation, m.
$x_s$	$x$ coordinate of the flow separation point, m.
$\xi$	nondimensional distance away from the separation point (equal to $(x - x_s)/H_b$ ).
$z$	vertical coordinate, m.
$z_b$	bed elevation, m.
$z_{sep}$	vertical position of the fitted separation streamline, m.
$z_{par}$	vertical position of the parameterized separation streamline, m.

[42] **Acknowledgments.** This work is supported by the Technology Foundation STW, the applied science division of NWO, and the technology program of the Ministry of Economic Affairs (project 06222). We are grateful for the data provided by Antoine Wilbers and Steve McLean and for the suggestions of Ralph Schielen. The constructive comments of Steve McLean, Jim Best, and an anonymous reviewer helped improve the manuscript significantly.

## References

- Allen, J. R. L. (1968), *Current Ripples: Their Relation to Patterns of Water and Sediment Motion*, pp. 161–182, North-Holland, Amsterdam.
- Bennett, S. J., and J. L. Best (1995), Mean flow and turbulence structure over fixed, two-dimensional dunes: Implications for sediment transport and bed form stability, *Sedimentology*, *42*, 491–513.
- Best, J. (2005), The fluid dynamics of river dunes: A review and some future research directions, *J. Geophys. Res.*, *110*, F04S02, doi:10.1029/2004JF000218.
- Best, J., and R. Kostaschuk (2002), An experimental study of turbulent flow over a low-angle dune, *J. Geophys. Res.*, *107*(C9), 3135, doi:10.1029/2000JC000294.
- Buckles, J., T. J. Hanratty, and R. J. Adrian (1984), Turbulent flow over large-amplitude wavy surfaces, *J. Fluid Mech.*, *140*, 27–44.
- Engel, P. (1981), Length of flow separation over dunes, *J. Hydraul. Div. Am. Soc. Civ. Eng.*, *107*, 1133–1143.
- Etheridge, D. W., and P. H. Kemp (1978), Measurements of turbulent flow downstream of a rearward-facing step, *J. Fluid Mech.*, *86*(3), 545–566.
- Fernandez, R., J. Best, and F. López (2006), Mean flow, turbulence structure, and bed form superimposition across the ripple-dune transition, *Water Resour. Res.*, *42*, W05406, doi:10.1029/2005WR004330.
- Giri, S., and Y. Shimizu (2006), Numerical computation of sand dune migration with free surface flow, *Water Resour. Res.*, *42*, W10422, doi:10.1029/2005WR004588.
- Hulscher, S. J. M. H. (1996), Tidal-induced large-scale regular bed form patterns in a three-dimensional shallow water model, *J. Geophys. Res.*, *101*, 20,727–20,744.
- Hulscher, S. J. M. H., and C. M. Dohmen-Janssen (2005), Introduction to special section on Marine Sand Wave and River Dune Dynamics, *J. Geophys. Res.*, *110*, F04S01, doi:10.1029/2005JF000404.
- Jerolmack, D. J., and D. C. Mohrig (2005), A unified model for subaqueous bed form dynamics, *Water Resour. Res.*, *41*, W12421, doi:10.1029/2005WR004329.
- Julien, P. Y., G. J. Klaassen, W. B. M. Ten Brinke, and A. W. E. Wilbers (2002), Case study: Bed resistance of Rhine River during 1998 flood, *J. Hydraul. Eng.*, *128*, 1042–1050.
- Korrmann, B. A. (1995), The effect of changes in the lee shape of dunes on the flow field, turbulence, and hydraulic roughness, *Rep. Meas. R 95-1*, Univ. of Utrecht, Utrecht, Netherlands.
- Kostaschuk, R., and P. Villard (1996), Flow and sediment transport over large subaqueous dunes: Fraser River, Canada, *Sedimentology*, *43*, 849–863.
- Kroy, K., G. Sauermaun, and H. J. Herrmann (2002), Minimal model for aeolian sand dunes, *Phys. Rev. E*, *66*(3), 1–18.
- Maddux, T. B., J. M. Nelson, and S. R. McLean (2003a), Turbulent flow over three-dimensional dunes: 1. Free surface and flow response, *J. Geophys. Res.*, *108*(F1), 6009, doi:10.1029/2003JF000017.
- Maddux, T. B., S. R. McLean, and J. M. Nelson (2003b), Turbulent flow over three-dimensional dunes: 2. Fluid and bed stresses, *J. Geophys. Res.*, *108*(F1), 6010, doi:10.1029/2003JF000018.
- McLean, S. R., S. R. Wolfe, and J. M. Nelson (1999), Spatially averaged flow over a wavy boundary revisited, *J. Geophys. Res.*, *104*, 15,743–15,753.
- Nakagawa, H., and I. Nezu (1987), Experimental investigation on turbulent structure of backward-facing step flow in an open channel, *J. Hydraul. Res.*, *25*, 67–88.
- Nelson, J. M., S. R. McLean, and S. R. Wolfe (1993), Mean flow and turbulence fields over two-dimensional bed forms, *Water Resour. Res.*, *29*, 3935–3954.
- Nelson, J. M., R. L. Shreve, S. R. McLean, and T. Drake (1995), Role of near-bed turbulence structure in bed load transport and bed form mechanics, *Water Resour. Res.*, *31*, 2071–2086.
- Nelson, J. M., A. R. Burman, Y. Shimizu, S. R. McLean, R. L. Shreve, and M. Schmeeckle (2005), Computing flow and sediment transport over bedforms, in *Proceedings of the 4th IAHR Symposium on River, Coastal, and Estuarine Morphodynamics, 4–7 October 2005, Urbana, Illinois, USA*, vol. 2, edited by G. Parker and M. H. Garcia, pp. 861–872, Taylor and Francis, London.
- Niño, Y., A. Atala, M. Barahona, and D. Aracena (2002), Discrete particle model for analyzing bedform development, *J. Hydraul. Eng.*, *128*, 381–389.
- Ogink, H. J. M. (1988), Hydraulic roughness of bedforms, *Rep. M2017*, Delft Hydraul., Delft, Netherlands.
- Onda, S., and T. Hosoda (2004), Numerical simulation on development process of dunes and flow resistance, in *Proceedings of Second International Conference on Fluvial Hydraulics, 23–25 June 2004, Napoli, Italy*, vol. 1, edited by M. Greco, A. Carravetta, and R. Della Morte, pp. 245–252, Balkema, Leiden, Netherlands.
- Paarlberg, A. J., C. M. Dohmen-Janssen, S. J. M. H. Hulscher, and A. P. P. Termes (2005), A parameterization for flow separation in a river dune development model, in *Proceedings of the 4th IAHR Symposium on River, Coastal, and Estuarine Morphodynamics, 4–7 October 2005, Urbana, Illinois, USA*, vol. 2, edited by G. Parker and M. H. Garcia, pp. 883–895, Taylor and Francis, London.
- Paarlberg, A. J., C. M. Dohmen-Janssen, S. J. M. H. Hulscher, J. Van den Berg, and A. P. P. Termes (2006), Modelling morphodynamic evolution of river dunes, in *Proceedings of the International Conference on Fluvial Hydraulics, 6–8 September 2006, Lisbon, Portugal*, edited by R. M. L. Ferreira et al., pp. 969–978, Taylor and Francis, London.
- Raudkivi, A. J. (1963), Study of sediment ripple formation, *J. Hydraul. Div. Am. Soc. Civ. Eng.*, *89*, 15–33.
- Schatz, V., and H. J. Herrmann (2006), Flow separation in the lee side of transverse dunes: A numerical investigation, *Geomorphology*, *81*, 207–216, doi:10.1016/j.geomorph.2006.04.009.
- Smith, J. D., and S. R. McLean (1977), Spatially averaged flow over a wavy surface, *J. Geophys. Res.*, *82*, 1735–1746.
- Sumer, B. M., L. H. C. Chua, N. S. Cheng, and J. Fredsøe (2003), Influence of turbulence on bed load sediment transport, *J. Hydraul. Eng.*, *129*, 585–596.
- Termes, A. P. P. (1984), Water movement over a horizontal bed and solitary sand dune, *Rep. R/1984/H/8*, Delft Univ. of Technol., Delft, Netherlands.
- Tjerry, S., and J. Fredsøe (2005), Calculation of dune morphology, *J. Geophys. Res.*, *110*, F04013, doi:10.1029/2004JF000171.
- Van den Berg, J., and R. Van Damme (2005), Sand wave simulation on large domains, in *Proceedings of the 4th IAHR Symposium on River, Coastal, and Estuarine Morphodynamics, 4–7 October 2005, Urbana, Illinois, USA*, vol. 2, edited by G. Parker and M. H. Garcia, pp. 991–997, Taylor and Francis, London.
- Van Mierlo, M. C. L. M., and J. C. C. De Ruiter (1988), Turbulence measurements above artificial dunes: Report on measurements, *Rep. Q789*, WL Delft Hydraul., Delft, Netherlands.

- Vanoni, V. A., and L. S. Hwang (1967), Relation between bed forms and friction in streams, *J. Hydraul. Div. Am. Soc. Civ. Eng.*, 93, 121–144.
- Venditti, J. G. (2007), Turbulent flow and drag over fixed two- and three-dimensional dunes, *J. Geophys. Res.*, 112, F04008, doi:10.1029/2006JF000650.
- Walker, I. J., and W. G. Nickling (2002), Dynamics of secondary airflow and sediment transport over and in the lee of transverse dunes, *Prog. Phys. Geogr.*, 26(1), 47–75, doi:10.1191/0309133302pp325ra.
- Wijbenga, J. H. A. (1990), Flow resistance and bedform dimensions for varying flow conditions: A literature review, *TOW Rivers Rep. Q785*, WL Delft Hydraul., Delft, Netherlands.

---

C. M. Dohmen-Janssen, S. J. M. H. Hulscher, and A. J. Paarlberg, Department of Water Engineering and Management, University of Twente, Horst Building, P.O. Box 217, NL-7500 ABE, Enschede, Netherlands. (c.m.dohmen-janssen@utwente.nl; s.j.m.h.hulscher@utwente.nl; a.j.paarlberg@utwente.nl)

P. Termes, HKV Consultants, P.O. Box 2120, NL-8203 AC, Lelystad, Netherlands. (paul.termes@hkv.nl)